Journal of Physical Science, Vol. 34(2), 59–73, 2023

Synthesis and Characterisation of ZnO/Ag Nanocomposites Prepared via Green Method Using Pineapple Peel Extract for Photocatalytic Enhancement in Degrading Methylene Blue Dye Solutions

Ari Sulistyo Rini,[1*] Rahmi Dewi,[1] Jasril,[2] Tessa Marshanda,[1] Yolanda Rati[3] and Yan Soerbakti[1]

[1]Department of Physics, Faculty of Mathematics and Natural Sciences, Universitas Riau, St. H.R. Soebrantas, KM. 12.5, Pekanbaru, Riau 28293, Indonesia
[2]Department of Chemistry, Faculty of Mathematics and Natural Sciences, Universitas Riau, St. H.R. Soebrantas, KM. 12.5, Pekanbaru, Riau 28293, Indonesia
[3]Department of Physics, Faculty of Mathematics and Natural Sciences, Institut Teknologi Bandung, St. Ganesa, No.10, Bandung, West Java 40132, Indonesia

[*]Corresponding author: ari.sulistyo@lecturer.unri.ac.id

Published online: 25 August 2023

To cite this article: Rini, A. S. et al. (2023). Synthesis and characterisation of ZnO/Ag nanocomposites prepared via green method using pineapple peel extract for photocatalytic enhancement in degrading methylene blue dye solutions. *J. Phys. Sci.*, 34(2), 59–73. https://doi.org/10.21315/jps2023.34.2.5

To link to this article: https://doi.org/10.21315/jps2023.34.2.5

ABSTRACT: *Photocatalytic is one of the technological developments of renewable materials in overcoming water pollution due to industrial waste treatment. In this study, photocatalytic observations were carried out with a methylene blue (MB) degradation approach using zinc oxide and silver (ZnO/Ag) nanocomposites (NCs) which were enhanced by a new green synthesis in the form of pineapple peel extract (Ananas comosus) as a bio-stabiliser. The amount of Ag was varied by 5%, 10% and 15%. UV-Vis spectroscopy (UV-Vis), X-ray diffrection (XRD) and scanning electron microscopy-energy dispersive X-ray analysis (SEM-EDX) spectroscopy were analysed to study the optical properties, structure, morphology and composition of the samples. The characterisation results show that the absorption peak occurs in the 359 nm to 368 nm region with a band gap energy of 2.96 eV to 3.00 eV. Based on the XRD pattern, a hexagonal wurtzite structure was obtained with a crystal size of 18.37 nm. The particle morphology shows a flower-like shape with an average diameter of 60 nm. The EDX spectrum confirmed the elemental content of Zn, oxygen (O) and Ag. The photocatalytic activity showed that 10% ZnO/Ag was able to optimally degrade MB (10 ppm) with a reaction rate constant of 0.0091 min^{-1}. Therefore, ZnO/Ag NCs were proven to be able to degrade dyes faster than pure ZnO.*

Keywords: methylene blue, nanocomposites, pineapple (*Ananas comosus*), photocatalytic, ZnO/Ag

1. INTRODUCTION

The increasing demand for clothing and food has affected large-scale industrial development. In addition, it also causes environmental pollution, especially due to dye waste. These substances are often the main cause of declining water quality, causing damage to the ecosystem.[1] The use of photocatalysts is an effective way to overcome these problems. Photocatalysts utilise light energy into chemical energy which in the process occurs a redox reaction with organic compounds so that the liquid waste can become clear water again.[2] In general, photocatalyst activity testing is carried out by utilising the wide band gap energy in the semiconductor material. Several types of inorganic metal oxides have been researched and investigated in recent years such as zinc oxide (ZnO), titanium dioxide (TiO_2) and copper (II) oxide (CuO).[3] ZnO is a nanomaterial that is often studied because it has chemical stability and the ability to absorb UV radiation is very high, can survive at room temperature and is sensitive to light. In addition, ZnO is non-toxic, relatively inexpensive, not easily damaged, resistant to high temperatures and transparent in the visible light area.[4]

Pure ZnO semiconductors without doping or other composite materials have poor electrical characteristics i.e., a low conductivity value of 6.24×10^{-7} S/m.[5] Silver (Ag), manganese (Mn), gallium (Ga), aluminum (Al) and copper (Cu) are commonly used as impurities to ZnO. Nanocomposites (NCs) between semiconductor and Ag has strong potential to overcome the weakness of ZnO conductivity. It is known that Ag proved to be effective for p-type ZnO synthesis because it can increase the conductivity as a result of its congenital defects such as oxygen (O) deficiency and Zn interstitial.[6] In addition, Ag is a promising material in health and environmental applications, such as antiseptic additives in packaging or textiles, antibacterial in medical devices, tile coating materials and water purification systems.[1] The addition of Ag can increase the photocatalytic activity of ZnO because it inhibits the electron-hole recombination process due to a large number of trapped electrons.[7] Therefore, these ZnO and Ag nanoparticles (NPs) can be regarded as NCs that can be applied as efficient photocatalysts against pollutants polluting liquid waste.

Nanoparticles are produced by several methods i.e., physically (top-down): laser light irradiation and evaporation or condensation and chemically (bottom-up): sol-gel, metal ion reduction and metal agglomeration.[8] These methods can damage the environment because of the use of toxic solvents, high energy consumption and emitting hazardous waste.[9] Therefore, it is necessary to develop methods that are more environmentally friendly. The green synthesis of NPs using plant extracts has been widely studied. The utilisation of this plant acts as a reducing agent

because of the content of secondary metabolites or antioxidants.[10] Flavonoids are phenolic compounds that have antioxidant properties that can reduce metal ions and prevent free radicals that damage cells.[11]

In this study, ZnO/Ag NCs were prepared using the green-synthesis method. Pineapple rind was chosen as a reductant because it has higher total phenolic and flavonoid content compared to other parts.[12] The utilisation of pineapple peel is also an alternative solution to reducing waste in the environment, which is mostly found in the market. The effect of Ag composition on ZnO was studied on its physical properties and applied as a photocatalyst to degrade the pollutant methylene blue.

2. MATERIALS AND METHODS

2.1 Green Synthesis of ZnO

Extract preparation was carried out as in our previous study, where all the materials used were purchased in Indonesia and the synthesis process was carried out at the Material Physics Laboratory, University of Riau.[13] Fifty milliliters of pineapple peel extract and 50 ml of $Zn(NO_3)_2 \cdot 6H2O$ (50 mM) were homogenised for 30 min. NaOH 5 M was added to the solution until pH of 12 was reached for stabilisation. Then, this solution was heated in a microwave oven for 2 min (360 Watts). The precipitate obtained was centrifuged at 4,000 rpm for 10 min, washed three times and dried at 110°C using hotplate.

2.2 Preparation of ZnO/Ag Nanocomposites

One gram of synthesised ZnO was dissolved in 50 ml of demineralised water. $AgNO_3$ powder and pineapple peel extract were added to the solution successively and then stirred until homogeneous. The mass percentage of $AgNO_3$ was varied, 5%, 10% and 15%. The solution was irradiated in the same way as ZnO using a microwave oven with a power of 360 Watts for 2 min.

2.3 Measurement

Optical absorption, diffraction pattern, morphology and elemental composition of ZnO/Ag NCs were characterised using SHIMADZU UV-Vis spectrophotometer (Agilent Technologies, Malaysia, G68860A), X'Pert PRO type diffractometer and Hitachi Flexsem 100 (SEM-EDX) instrument.

2.4 Evaluation of Photocatalytic

ZnO/Ag NCs 1 g was dispersed into 10 ppm methylene blue (MB) solution. This solution was stirred using a magnetic stirrer for 1 h in the dark to get adsorption-desorption equilibrium. Then, it is irradiated by four UV-C lamps (8 Watts) during the degradation process. The MB concentration at 664 nm was determined from the absorbance peak of MB at 664 nm using the UV-Vis spectrophotometer characterisation. The percentage degradation of MB is calculated using the formula:

$$MB\ degradation\ (\%) = \frac{C_0 - C_t}{C_0} \times 100\,\% \quad (1)$$

where C_0 is the initial MB concentration and C_t is the MB concentration after time t.

3. RESULTS AND DISCUSSION

3.1 Absorption Properties

The formation of ZnO NPs was confirmed by optical absorption peaks in the UV and visible light areas. The UV-Vis absorption curve with a wavelength function can be seen in Figure 1.

The absorption peaks of ZnO, ZnO/Ag 5%, ZnO/Ag 10% and ZnO/Ag 15% were at 359 nm, 362 nm, 365 nm and 368 nm, respectively. The presence of the absorption peak is in the UV region which is in accordance with previous studies at 362 nm.[14] The addition of metal Ag affects the optical properties of ZnO. The absorption intensity of ZnO/Ag NCs is higher than that of pure ZnO. This is due to the increasing number of constituent atoms thereby increasing the absorbance ability. The absorption peak shifts towards a larger wavelength as the mass percentage of Ag increases. This indicates that the band gap is getting smaller so that the energy required by the molecule is getting lower.[15] The band gap energy is determined by the Tauc plot method seen in Figure 2.

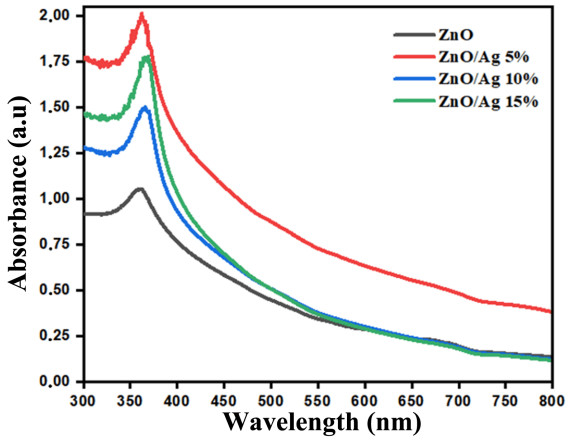

Figure 1: UV-Vis absorption spectrum.

The band gap energy decreases with the addition of Ag metal to ZnO. The substitution of Ag metal results in a decrease in the band gap distance so that the energy required for electron excitation also decreases.[16] Therefore, ZnO/Ag is expected to increase photocatalytic activity by increasing the number of electrons in the conduction band.

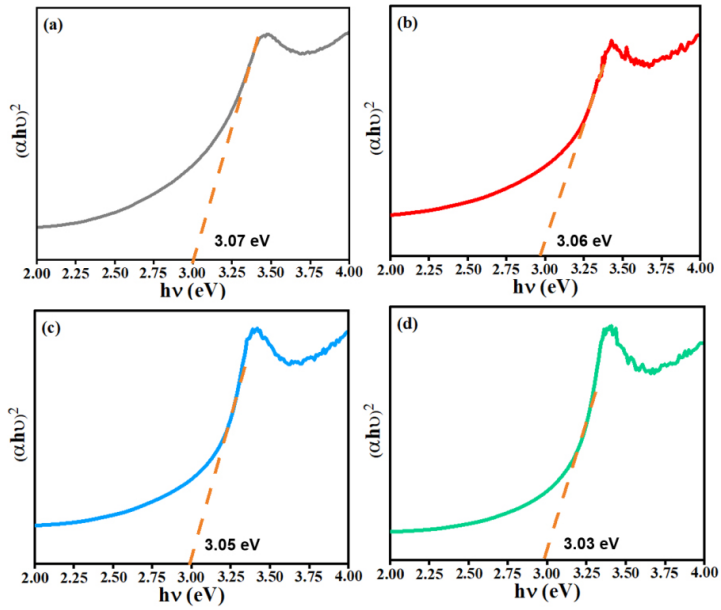

Figure 2: The bandgap energy in pure ZnO and variation of ZnO/Ag NCs.

3.2 Structure Properties

The X-ray diffraction (XRD) spectra of ZnO and ZnO/Ag can be seen in Figure 3. The XRD pattern shows that there are seven diffraction peaks with different intensities. The diffraction peak is at 2θ = 31.75°, 34.40°, 36.23°, 47.51°, 56.55°, 62.91° and 67.95° with the orientation planes (101), (002), (101), (012), (110), (013) and (112), respectively. The analysis of this diffraction peak is in accordance with the Inorganic Crystal Structure Database (ICSD) data number 98-002-7791.[17]

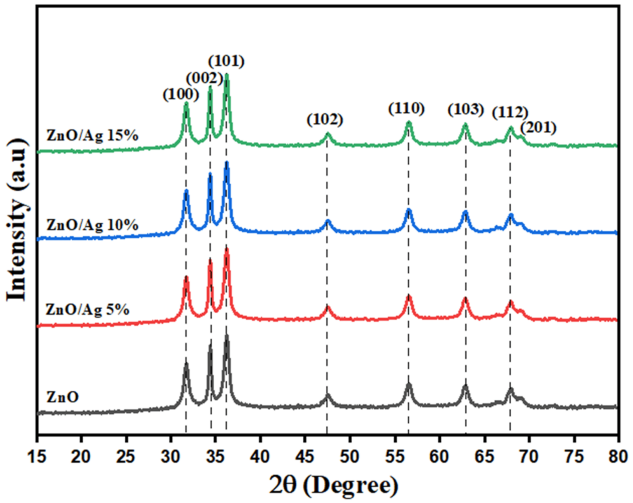

Figure 3: XRD pattern of ZnO/Ag NCs.

The diffraction pattern shows that the crystal phase of pure ZnO and ZnO/Ag is a hexagonal wurtzite structure. The diffraction intensity decreases with the addition of Ag mass on ZnO. In addition, there is also a shift in the diffraction peak towards a larger angle. This is due to the substitution of Ag ions that enter and replace Zn ions without changing the hexagonal structure of ZnO.[18] The lattice parameters a and c were determined using the diffraction peaks of (100) and (002) planes as seen in Table 1. The value of a and c decreases with the addition of Ag mass in ZnO. This is due to the presence of Zn ions which are replaced by Ag ions which have different atomic radii. Therefore, it affects the length and position of the bond between the metal and O in the crystal lattice of the NPs.[19] The crystallite size is calculated using the Scheerer equation. Based on Table 1, it can be seen that the crystallite size of ZnO is smaller than that of ZnO/Ag, 16.35 nm. The increasing crystallite size indicates a high crystalline level because of the more constructive interference that occurs and also because more and more ions are substituted along with the addition of Ag metal.[20]

Table 1: Lattice parameter and crystallite size of ZnO/Ag nanocomposites.

Sample	2θ (°)	Interplanar spacing (Å)	Lattice parameter		Crystallite size (nm)
			a = b (Å)	c (Å)	
ZnO	31.735	2.607	3.253	5.213	16.35
ZnO/Ag 5%	31.809	2.603	3.247	5.206	18.37
ZnO/Ag 10%	31.809	2.603	3.247	5.206	18.12
ZnO/Ag 15%	31.728	2.606	3.258	5.212	18.37

3.3 Particles Morphology

Micrographs of pure ZnO and ZnO/Ag at a magnification of 10,000 times were identified by SEM characterisation presented in Figure 4.

There is not a significant difference in the morphology of ZnO particles and ZnO/Ag particles. ZnO is spherical and flower-shaped, while ZnO/Ag resembles a flower with the ends of the cluster increasingly conical. This is because in the formation of hexagonal ZnO aggregation occurs due to the large surface energy so that the particles grow in a certain direction.[21]

The presence of Ag composites in ZnO NPs has decreased the particle diameter where ZnO, ZnO/Ag 5%, ZnO/Ag 10% and ZnO/Ag 15% are 254 nm, 60 nm, 126 nm and 122 nm, respectively. On the other hand, increasing the mass percentage of Ag produces larger particles. This is due to the increased aggregation of the particles and the high concentration that causes the particles to bond to one another or stick together.[22] In addition, there are small crystals that are thought to be Ag ions attached to the ZnO surface which are spread unevenly. The results of this SEM micrograph are similar to the studies conducted by the previous report.[23]

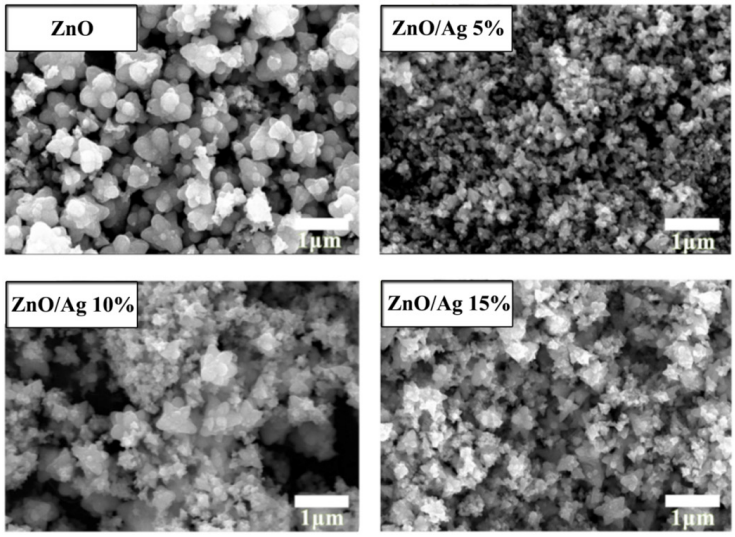

Figure 4: Micrographs for pure ZnO and different percentages of ZnO/Ag NCs.

3.4 Elemental Composition

The elemental compositions of pure ZnO and ZnO/Ag NCs were identified from the EDX Figure 5 spectrum. The elements detected were carbon (C), Zn, O, Cu, zirconium (Zr), argon (Ar) and Ag with different levels of atomic mass.

The highest percentage of Zn atoms is found in ZnO/Ag 15% at 65.66% and the lowest is ZnO/Ag 10% at 48.33%. The most detected elemental O content was found in 15% ZnO/Ag at 16.84% and the least found in ZnO/Ag 10% at 13.19%. The existence of elemental O comes from lattice O and from water molecules that are absorbed.[24] The EDX spectrum shows that the weight percentage of the element Ag increases with the increase in Ag metal. The highest composition of the element Ag is in the ZnO/Ag 15% sample at 1.85% and the lowest in the ZnO/Ag 10% sample at 1.06%. Elements of Ag atoms were not detected in ZnO/Ag 5% which may be due to the addition of a very small number of Ag atoms. The percentage of C elements is not much different from the distribution of Zn elements, where ZnO/Ag 10% contains 33.19% and the lowest is in ZnO/Ag 15% at 13.83%. The presence of element C is ascribed to the annealing process.[25]

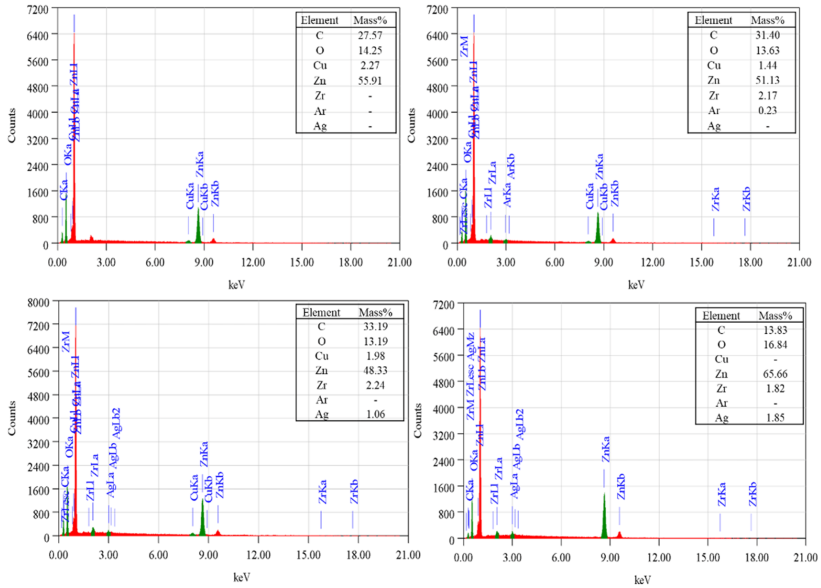

Figure 5: EDX spectrum in determining elemental composition.

The highest percentage of Cu, 2.27%, is found in pure ZnO and at least 1.44% in ZnO/Ag 5%. The elemental Cu is an element that is not present in ZnO/Ag 15%. The percentage of Zr element of 2.24% has the highest value at ZnO/Ag 10% and is an element that is not found in pure ZnO. The element Ar atom which is only found in the ZnO/Ag 5% sample with a percentage value of 0.23%. Elements other than Zn, O, Ag and C are most probably come from contaminated precursors of the sample characterisation holder.

3.5 Photocatalytic Activity

The ability of pure ZnO and ZnO/Ag NCs as photocatalyst for MB degradation was carried out under UV irradiation. The absorption comparison curves at time *t* and the initial absorption of the MB solution (664 nm) of each sample are presented in Figure 6(a). The ZnO curve looks higher and the decrease is not significant than the ZnO/Ag NCs. This shows that the degradation ability of pure ZnO is slower than of ZnO/Ag NCs. ZnO/Ag 10% showed the most significant decrease in the curve followed by ZnO/Ag 15% and ZnO/Ag 5%. The addition of the transition metal Ag has been shown to increase the number of electrons that

can be absorbed in the conduction band. The photogeneration process of electrons moving from the ZnO conduction band to Ag particles can increase the efficiency of the photocatalyst.[26]

Figure 6(b) shows the relationship between $\ln(A/A_0)$ with respect to time t with variations in the addition of Ag metal. The $\ln(A/A_0)$ curves of pure ZnO and ZnO/Ag 5% showed only slight differences and did not decrease significantly compared to the Ag 10% and Ag 15% composites. The reaction rates of pure ZnO and ZnO/Ag 5% were -1.4×10^{-3} min^{-1} and 1.7×10^{-3} min^{-1}, respectively. The degradation process using ZnO/Ag 10% shows fluctuations in the absorbance vs time curve. The $\ln(A/A_0)$ curve of ZnO/Ag 10% significantly decreased after 120 min of irradiation indicating that the degradation occurred faster with the highest reaction rate constant of -9.1×10^{-3} min^{-1}. The decrease in the $\ln(A/A_0)$ curve for ZnO/Ag 15% is quite significant without any increase. ZnO/Ag 15% has a reaction rate constant of -4.3×10^{-3} min^{-1}. The increase in the curve indicates the oxidation reaction in MB is faster than the reduction reaction (decreasing the curve) which caused by the unstable reaction.[27] The addition of Ag metal to ZnO improve the photocatalyst activity to be faster than pure ZnO. This is due to a decrease in the band gap energy where electrons are easily excited to the covalent band towards the surface of the semiconductor material so as to produce more hydroxyl radicals.[28]

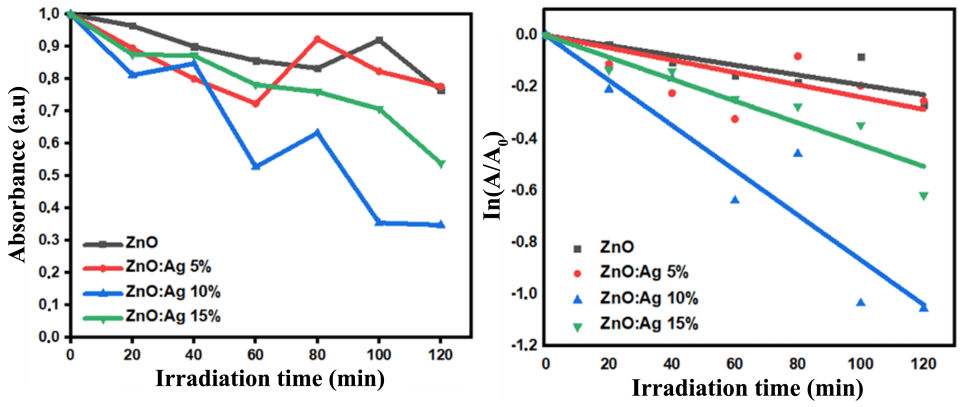

(a) (b)

Figure 6: (a) Absorbance of MB solution at λ = 664 nm and (b) the reaction rate of the first order kinetic mode.

The degradation of MB is indicated by a change in the colour of the solution becoming clearer (Figure 7[a]). This degradation process was confirmed by a significant decrease in the curves (Figures 6[a] and 6[b]) by the catalyst. MB degradation occurs because electrons in the sample are excited from the valence band to the conduction band, resulting in a vacancy or hole in the valence band. These electrons react with dissolved O to form superoxide radical anions (O^{-2}) which then react with H_2O molecules to form hydroxyl radicals and at the same time the unrecombined holes will react with H_2O to form hydroxyl radicals (OH^-) which are oxidising agents that MB.[2]

The degradation efficiency by pure ZnO catalyst and ZnO/Ag NCs can be seen in Figure 7(b). The highest percentage of MB degradation was 41.29% by ZnO/Ag 10% followed by ZnO/Ag 15%, ZnO/Ag 5% and pure ZnO samples at 24.41%, 17.64% and 12.69%, respectively. The ZnO/Ag 10% NCs was proven the optimum conditions for degrading MB which was more effective than other samples. Its condition due to this material has the highest reaction rate. The highest reaction rate of ZnO/Ag 10% is related to the metalic state of Ag disperse on the ZnO surfaces. Eventhough, there is no clear evidence to show the correlations between its activity to the structural, morphological and optical properties. The degradation at 15% Ag mass percentage decreased due to the large amount of Ag metal composition that covered the ZnO surface so that it inhibited the interaction between ZnO and incident light.[29] In addition, it may be due to light scattering and the appearance of bulk defects so that photocatalytic activity is diminished.[30] The addition of less Ag at 5% also experienced a lower degradation power due to the lack of Ag. This results in the inhibition of the process of excitation of electrons in the valence band and therefore the recombination of electron-hole occurs.[31] Overall, Ag NPs have succeeded in increasing the photocatalytic activity of ZnO semiconductors.

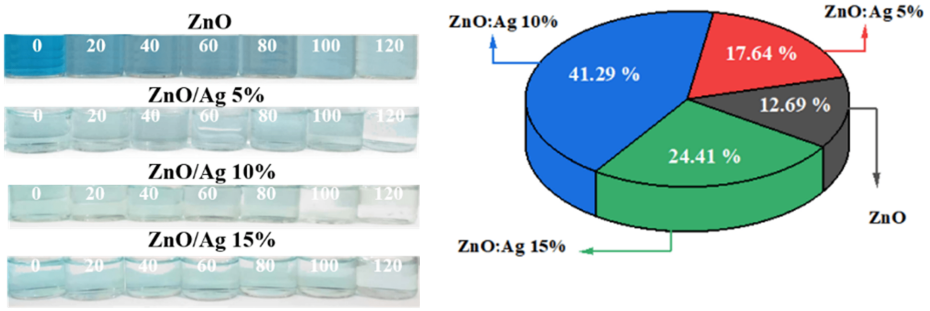

(a) (b)

Figure 7: (a) MB degradation process image and (b) photocatalytic efficiency of MB degradation.

In comparison, the ratio of reaction rate ZnO/Ag 10% on pure ZnO by microwave synthesis previously reported is twice, whereas in this work is six times.[32] Furthermore, the performance of Ag/ZnO recently published using hydrothermal microwave heating synthesis exhibit MB degradation efficiency of 40% for 5 h.[33] Compared to current work, it shows a shorter degradation time for MB degradation over 2 h.

4. CONCLUSION

The composite Ag metal has succeeded in increasing the photocatalytic activity of ZnO. The optical absorption increases and the band gap energy decreases of ZnO after the addition of Ag metal. Hexagonal structure was found in ZnO/Ag NCs with decreased diffraction intensity. In addition, the ZnO particle diameter was also reduced in the presence of Ag metal inserted in the ZnO structure. The distribution of elements in the ZnO/Ag NCs confirms the presence of Zn, O and Ag atoms. The degradation efficiency of ZnO/Ag NCs of 41.29% was higher than that of pure ZnO of 12.69%.

5. ACKNOWLEDGEMENTS

The authors would like to thank the Ministry of Education and Culture of the Republic of Indonesia and the LPPM of Universitas Riau for funding this research through DRTPM 2022 with contract number: 2597/UN19.5.1.3/PT.01.03/2022.

6. REFERENCES

1. Kowalska-Góralska, M. et al. (2015). Biocidal properties of silver-nanoparticles in water environments. *Pol. J. Environ. Stud.*, 24(4), 1641–1647. https://doi.org/10.15244/pjoes/39554
2. Fageria, P. et al. (2015). Graphitic-carbon nitride support for the synthesis of shape-dependent ZnO and their application in visible light photocatalysts. *RSC Adv.*, 5(98), 80397–80409. https://doi.org/10.1039/C5RA12463H
3. Nishikiori, H. et al. (2019). Formation of CuO on TiO_2 surface using its photocatalytic activity. *Catalysts*, 9(4), 1–12. https://doi.org/10.3390/catal9040383
4. Kumar, S. S. et al. (2013). Synthesis, characterization and optical properties of zinc oxide nanoparticles. *Int. Nano Lett.*, 3(1), 1–6. https://doi.org/10.1186/2228-5326-3-30
5. Rajendran, S. et al. (2016). Ce^{3+}-ion-induced visible-light photocatalytic degradation and electrochemical activity of ZnO/CeO_2 nanocomposite. *Sci. Rep.*, 6(1), 1–11. https://doi.org/10.1038/srep31641

6. Saravanan, R. et al. (2013). ZnO/Ag nanocomposite: An efficient catalyst for degradation studies of textile effluents under visible light. *Mater. Sci. Eng. C*, 33(4), 2235–2244. https://doi.org/10.1016/j.msec.2013.01.046
7. Zaleska, A. (2008). Doped-TiO_2: A review. *Recent Pat. Eng.*, 2(3), 157–164. https://doi.org/10.2174/187221208786306289
8. Saratale, R. G. et al. (2018). New insights on the green synthesis of metallic nanoparticles using plant and waste biomaterials: Current knowledge, their agricultural and environmental applications. *Environ. Sci. Pollut. Res.*, 25(11), 10164–10183. https://doi.org/10.1007/s11356-017-9912-6
9. Chandran, S. et al. (2016). Biosynthesis of PVA encapsulated silver nanoparticles. *J. Appl. Res. Technol.*, 14(5), 319–324. https://doi.org/10.1016/j.jart.2016.07.001
10. Kuppusamy, P. et al. (2016). Biosynthesis of metallic nanoparticles using plant derivatives and their new avenues in pharmacological applications–An updated report. *Saudi Pharm. J.*, 24(4), 473–484. https://doi.org/10.1016/j.jsps.2014.11.013
11. Awwad, A. M. et al. (2020). Green synthesis of zinc oxide nanoparticles (ZnO-NPs) using Ailanthus altissima fruit extracts and antibacterial activity. *Chem. Int.*, 6(3), 151–159. https://doi.org/10.5281/zenodo.3559520
12. Fitriyanti, F. et al. (2019). Antibacterial activity test of ethanol extract pineapple (Ananascomosus (L.) Merr.) peel against growth of Propionibacterium acnes. *Borneo J. Pharm.*, 2(2), 108–113. https://doi.org/10.5281/10.33084/bjop.v2i2.928
13. Rini, A. S. et al. (2021). Microwave-assisted biosynthesis and characterization of ZnO film for photocatalytic application in methylene blue degradation. *Commun. Sci. Technol.*, 6(2), 69–73. https://doi.org/10.21924/cst.6.2.2021.484
14. Rini, A. S. et al. (2021). Effect of pH on the morphology and microstructure of ZnO synthesized using Ananascomosuspeel extract. *J. Phys. Conf. Ser.*, 2019(1), 1–7. https://doi.org/10.1088/1742-6596/2019/1/012100
15. Conradie, M. M. et al. (2014). Immobilisation of iron tris (β-diketonates) on a two-dimensional flat amine functionalised silicon wafer: A catalytic study of the formation of urethane, from ethanol and a diisocyanate derivative. *Polyhedron*, 79, 52–59. https://doi.org/10.1016/j.poly.2014.04.054
16. Hidayat, A. et al. (2021). Synthesis and characterization of TiO_2/ZnO-Ag@ TiO_2 nanocomposite and their performance as photoanode of organic dye-sensitized solar cell. *Mater. Today: Proc.*, 44(3), 3395–3399. https://doi.org/10.1016/j.matpr.2020.11.862
17. Mohamad, A. A. et al. (2017). First-principles calculation on electronic properties of zinc oxide by zinc–air system. *J. King Saud Univ. Eng. Sci.*, 29(3), 278–283. https://doi.org/10.1016/j.jksues.2015.08.002
18. Abinaya, C. et al. (2016). Structural and optical characterization and efficacy of hydrothermal synthesized Cu and Ag doped zinc oxide nanoplate bactericides. *Mater. Chem. Phys.*, 184, 172–182. https://doi.org/10.1016/j.matchemphys.2016.09.039
19. Sutanto, H. et al. (2015). Synthesized of double layer thin film ZnO/ZnO: Ag by sol-gel method for direct blue 71 photodegradation. *Reaktor*, 15(3), 175–181. https://doi.org/10.14710/reaktor.15.3.175-181

20. Abdel-Galil, A. et al. (2015). Synthesis and characterization of Mn-doped ZnO diluted magnetic semiconductors. *Phys. B: Condens. Matter*, *477*, 20–28. https://doi.org/10.1016/j.physb.2015.08.001
21. Patil, S. S. et al. (2016). Green approach for hierarchical nanostructured Ag-ZnO and their photocatalytic performance under sunlight. *Catal. Today*, 260, 126–134. https://doi.org/10.1016/j.cattod.2015.06.004
22. Michen, B. et al. (2015). Avoiding drying-artifacts in transmission electron microscopy: Characterizing the size and colloidal state of nanoparticles. *Sci. Rep.*, 5(1), 1–7. https://doi.org/10.1038/srep09793
23. Chitradevi, T. et al. (2019). Structure, morphology and luminescence properties of sol-gel method synthesized pure and Ag-doped ZnO nanoparticles. *Mater. Res. Express*, 7(1), 1–11. https://doi.org/10.1088/2053-1591/ab5c53
24. Pirhashemi, M. & Habibi-Yangjeh, A. (2017). Ultrasonic-assisted preparation of plasmonic ZnO/Ag/Ag_2WO_4 nanocomposites with high visible-light photocatalytic performance for degradation of organic pollutants. *J. Colloid. Interface Sci.*, 491, 216–229. https://doi.org/10.1016/j.jcis.2016.12.044
25. Cheng, D. et al. (2021). Polydopamine-assisted in situ growth of three-dimensional ZnO/Ag nanocomposites on PET films for SERS and catalytic properties. *J. Mol. Liq.*, 338, 116639. https://doi.org/10.1016/j.molliq.2021.116639
26. Zhang, X. et al. (2017). Effects of Ag loading on structural and photocatalytic properties of flower-like ZnO microspheres. *Appl. Surf. Sci.*, 391, 476–483. https://doi.org/10.1016/j.apsusc.2016.06.109
27. Begum, R. et al. (2020). Chemical reduction of methylene blue in the presence of nanocatalysts: A critical review. *Rev. Chem. Eng.*, 36(6), 749–770. https://doi.org/10.1515/revce-2018-0047
28. Zhai, H. et al. (2015). Direct sunlight responsive Ag-ZnO heterostructure photocatalyst: Enhanced degradation of rhodamine B. *J. Phys. Chem. Solids*, 78, 35–40. https://doi.org/10.1016/j.jpcs.2014.11.004
29. Liu, Y. et al. (2019). Novel and efficient synthesis of Ag-ZnO nanoparticles for the sunlight-induced photocatalytic degradation. *Appl. Surf. Sci.*, 476, 632–640. https://doi.org/10.1016/j.apsusc.2019.01.137
30. Sharwani, A. A. et al. (2022). Photocatalytic degradation activity of goji berry extract synthesized silver-loaded mesoporous zinc oxide (Ag@ZnO) nanocomposites under simulated solar light irradiation. *Sci. Rep.*, 12(1), 1–18. https://doi.org/10.1038/s41598-022-14117-w
31. Yang, Y. et al. (2022). Oxygen-vacancy-induced O_2 activation and electron-hole migration enhance photothermal catalytic toluene oxidation. *Cell Rep. Phys. Sci.*, 3(8), 1–19. https://doi.org/10.1016/j.xcrp.2022.101011
32. Chakraborty, U. et al. (2021). Microwave-assisted assembly of Ag_2O-ZnO composite nanocones for electrochemical detection of 4-Nitrophenol and assessment of their photocatalytic activity towards degradation of 4-Nitrophenol and Methylene blue dye. *J. Hazard Mater.*, 416, 1–17. https://doi.org/10.1016/j.jhazmat.2021.125771

33. Xin, Z. et al. (2018). Microwave-assisted hydrothermal synthesis of chrysanthemum-like Ag/ZnO prismatic nanorods and their photocatalytic properties with multiple modes for dye degradation and hydrogen production. *RSC Adv.*, 8(11), 6027–6038. https://doi.org/10.1039/C7RA12097D